Geochemistry Geophysics Geosystems G3
AN ELECTRONIC JOURNAL OF THE EARTH SCIENCES
Published by AGU and the Geochemical Society

Article
Volume 2
July 31, 2001
Paper number 2000GC000146
ISSN: 1525-2027

Thermal fractionation of air in polar firn by seasonal temperature gradients

Jeffrey P. Severinghaus and Alexi Grachev
Scripps Institution of Oceanography, University of California, San Diego, La Jolla, California 92093-0244, USA (jseveringhaus@ucsd.edu)

Mark Battle
Department of Physics and Astronomy, Bowdoin College, 8800 College Station, Brunswick, Maine 04011-8488, USA (mbattle@bowdoin.edu)

[1] **Abstract:** Air withdrawn from the top 5–15 m of the polar snowpack (firn) shows anomalous enrichment of heavy gases during summer, including inert gases. Following earlier work, we ascribe this to thermal diffusion, the tendency of a gas mixture to separate in a temperature gradient, with heavier molecules migrating toward colder regions. Summer warmth creates a temperature gradient in the top few meters of the firn due to the thermal inertia of the underlying firn and causes gas fractionation by thermal diffusion. Here we explore and quantify this process further in order to (1) correct for bias caused by thermal diffusion in firn air and ice core air isotope records, (2) help calibrate a new technique for measuring temperature change in ice core gas records based on thermal diffusion [*Severinghaus et al.*, 1998], and (3) address whether air in polar snow convects during winter and, if so, whether it creates a rectification of seasonality that could bias the ice core record. We sampled air at 2-m-depth intervals from the top 15 m of the firn at two Antarctic sites, Siple Dome and South Pole, including a winter sampling at the pole. We analyzed $^{15}N/^{14}N$, $^{40}Ar/^{36}Ar$, $^{40}Ar/^{38}Ar$, $^{18}O/^{16}O$ of O_2, O_2/N_2, $^{84}Kr/^{36}Ar$, and $^{132}Xe/^{36}Ar$. The results show the expected pattern of fractionation and match a gas diffusion model based on first principles to within 30%. Although absolute values of thermal diffusion sensitivities cannot be determined from the data with precision, relative values of different gas pairs may. At Siple Dome, $\delta^{40}Ar/4$ is 66 ± 2% as sensitive to thermal diffusion as $\delta^{15}N$, in agreement with laboratory calibration; $\delta^{18}O/2$ is 83 ± 3%, and $\delta^{84}Kr/48$ is 33 ± 3% as sensitive as $\delta^{15}N$. The corresponding figures for summer South Pole are 64 ± 2%, 81 ± 3%, and 34 ± 3%. Accounting for atmospheric change, the figure for $\delta O_2/N_2/4$ is 90 ± 3% at Siple Dome. Winter South Pole shows a strong depletion of heavy gases as expected. However, the data do not fit the model well in the deeper part of the profile and yield a systematic drift with depth in relative thermal diffusion sensitivities (except for Kr, constant at 34 ± 4%), suggesting the action of some other process that is not currently understood. No evidence for wintertime convection or a rectifier effect is seen.

Keywords: Thermal diffusion; firn air; isotope fractionation; gas isotopes; paleothermometer; thermal diffusion sensitivity.

Index terms: Troposphere—constituent transport and chemistry; global change—atmosphere; glaciology; paleoclimatology.

Received January 31, 2001; **Revised** May 7, 2001; **Accepted** May 8, 2001; **Published** July 31, 2001.

Severinghaus, J. P., A. Grachev, and M. Battle, 2001. Thermal fractionation of air in polar firn by seasonal temperature gradients, *Geochem. Geophys. Geosyst.*, vol. 2, Paper number 2000GC000146 [10,036 words, 7 figures, 3 tables]. Published July 31, 2001.

1. Introduction

[2] The porous and permeable layer of snow on top of polar ice sheets is typically 50–100 m thick and is known as the firn layer. At the base of this layer the firn is continuously transformed into impermeable ice, trapping air in bubbles. The air in firn mixes slowly with the atmosphere, primarily by molecular diffusion [*Schwander et al.*, 1988]. Consequently, the mean age of the air (defined as the time elapsed since the air crossed the surface) increases downward in the firn and reaches several decades at sites with thick firn [*Schwander et al.*, 1993].

[3] A number of recent studies have exploited this fact to reconstruct atmospheric concentration histories of various gases, such as halocarbons [*Butler et al.*, 1999], O_2/N_2 ratios and N_2O [*Battle et al.*, 1996], and ^{13}C of CO_2 [*Francey et al.*, 1999]. Other recent studies have taken advantage of the fact that temperature gradients in the firn arising from rapid climate variation cause isotope fractionation of nitrogen and argon gas by the process of thermal diffusion [*Severinghaus et al.*, 1998; *Leuenberger et al.*, 1999; *Severinghaus and Brook*, 1999; *Lang et al.*, 1999]. This thermally driven fractionation results in an isotope anomaly in the deep firn air that is captured and preserved in air bubbles as the firn becomes ice, creating a marker of rapid temperature change events in the ice core paleoclimatic record. The magnitude of the isotope anomaly is proportional to the magnitude of the abrupt warming, so the amount of warming at fast climatic transitions may be quantified [*Severinghaus et al.*, 1998; *Severinghaus and Brook*, 1999]. Interpreting these thermally driven anomalies depends on laboratory calibration in which air is equilibrated in a known temperature gradient and the resulting isotope fractionation is measured (A. Grachev and J. P. Severinghaus, Calibration of the newly developed gas-phase paleothermometer: Fractionation of $^{15}N^{14}N$ and $^{14}N^{14}N$ by thermal diffusion, manuscript in preparation, 2001)(hereinafter referred to as Grachev and Severinghaus, manuscript in preparation, 2001). Snow is not used as the equilibration medium in these laboratory experiments, however, so it would be desirable to test the method in a more realistic setting such as polar firn.

[4] Here we describe modern isotope fractionation in the firn that occurs in response to seasonal temperature variations and use it to test the validity and accuracy of the thermal diffusion paleotemperature indicator. At many polar sites, surface temperature varies by >30°C seasonally. This creates strong temperature gradients in the top few meters of the firn owing to the fact that the firn at ~10 m depth closely maintains the mean annual temperature at all times [*Paterson*, 1969]. Theory [*Grew and Ibbs*, 1952] predicts that these gradients will lead to a characteristic pattern of thermally fractionated gases in the upper ~15 m of the firn column. A model of heat and gas diffusion in the firn enables a precise numerical prediction of the magnitude and shape of this pattern, when forced with the known surface temperature history. Air samples withdrawn from the shallow firn at two Antarctic sites, South Pole and Siple Dome, were then analyzed and compared with the model prediction. The agreement of model and

theory supports the use of the thermal diffusion paleoindicator. A wintertime sampling at South Pole was also made to verify that the reverse temperature gradient in winter creates the expected negative isotope anomaly. The results also have relevance to firn air studies that reconstruct atmospheric histories of gases such as O_2/N_2 [*Battle et al.*, 1996], ^{13}C of CH_4, and ^{13}C of CO_2 [*Francey et al.*, 1999], as these species may be significantly affected by thermal fractionation in response to seasonal temperature gradients or the geothermal gradient in the firn.

2. Diffusion Model

[5] We start by constructing a time-dependent numerical model of gas composition in the firn, which is driven by temperatures from a separate heat diffusion model. For simplicity, we neglect convective transport, although the top few meters of the firn may be ventilated by wind pumping and other convective processes [*Colbeck*, 1989; *Sowers et al.*, 1992]. We shall revisit this simplification later. The model has no adjustable parameters and thus serves as a stringent test of our understanding of the physical processes governing gas-isotope ratios in shallow firn.

[6] The transport of gas in polar firn is commonly modeled with the one-dimensional diffusion equation [*Schwander et al.*, 1993; *Battle et al.*, 1996; *Trudinger et al.*, 1997]. Here we modify the equation of *Schwander et al.* [1993] to include a term for thermal fractionation, in addition to their term for gravitational settling:

$$\frac{\partial C}{\partial t} = \frac{\partial}{\partial z}\left(D(z,T)\left[\frac{\partial C}{\partial z} - \frac{\triangle mg}{RT} + \Omega\frac{dT}{dz}\right]\right), \quad (1)$$

where C is the isotope delta value (e.g., $\delta^{15}N$), t is time, z is depth, D is the effective molecular diffusivity of gas in porous snow, T is temperature (in K), Δm is mass difference between isotopes, g is gravitational acceleration, R is the gas constant, and Ω is the thermal diffusion sensitivity (in ‰ K^{-1}). The gravitational settling term is $\Delta mg/RT$, and the thermal diffusion term is $\Omega(dT/dz)$.

[7] In concept, the diffusive flux of gas is driven by the difference between the existing isotopic gradient and the isotopic gradient under gravitational and thermal equilibrium. Thus the isotope values "relax" back to the equilibrium gradients, at a speed controlled by the diffusivity of gas in snow. Justification for this approach is discussed by *Bender et al.* [1994a] and relies on the observation that thermal diffusion proceeds at the speed of ordinary diffusion [*Chapman and Dootson*, 1917].

[8] The effective molecular diffusivity is estimated from an empirical diffusivity-density relation that was developed from observed CO_2 concentrations in South Pole firn air by *Battle et al.* [1996] and is scaled by the ratio of the free-air diffusivity of the model gas to that of CO_2. Free-air diffusivity $D_{\text{free air}}$ is calculated by the method of Fuller et al. as given by *Reid et al.* [1977], and the minor isotope (e.g., $^{29}N_2$ or ^{36}Ar) diffusivity into air is used (Table 1). The resulting effective diffusivities are close to those obtained independently using the relation of *Schwander et al.* [1988] and *Fabre et al.* [2000]. The density profile is modeled from *Herron and Langway* [1980], using the site parameters given in Table 2. Temperature and pressure corrections are as those given by *Schwander et al.* [1988]. The final expression for effective diffusivity D is

$$\frac{D}{D^{298.15\,\text{K},1\,\text{atm}}_{\text{free air}}} = \frac{1013.25}{P} \times \left(\frac{T}{298.15}\right)^{1.85}\left[2.00\left(1-\frac{\rho}{\rho_{\text{ice}}}\right) - 0.167\right], \quad (2)$$

where P is site surface pressure (in hPa), ρ is firn bulk density, and ρ_{ice} is ice density (917 kg m^{-3}).

Table 1. Parameters Used in the Diffusion Model and Derived From Firn Air Observations

Parameter	Value						
	$\delta^{15}N$	$\delta^{40}Ar$	$\delta^{18}O$	$\delta O_2/N_2$	$\delta^{84}Kr$	$\delta^{132}Xe$	CO_2
Δm	1	4	2	4	48	96	
Thermal Diffusion Sensitivities Used in the Diffusion Model							
Ω at 255 K[a]	+0.0150	+0.0387	+0.0249	+0.0538	+0.207	+0.300	
Ω at 230 K[a]	+0.0145	+0.0375			+0.201	+0.291	
Ω at 216 K[a]	+0.0141	+0.0364			+0.195	+0.283	
Error used in Monte Carlo	±0.0004					±0.02	
$D_{free\ air}10^{-5}$ m^2 s^{-1} at 298.15 K, 1013.25 hPa[b]	1.963	1.904	1.969	1.997	1.465	1.260	1.574
Relative Thermal Diffusion Sensitivities Derived From Firn Air Observations, %							
$\Omega/(\Omega^{15}\Delta m)$ at 255 K	100	66 ± 2	83 ± 3	90 ± 3	33 ± 3		
$\Omega/(\Omega^{15}\Delta m)$ at 230 K	100	64 ± 2	81 ± 3		34 ± 3		
$\Omega/(\Omega^{15}\Delta m)$ at 216 K	100				34 ± 4		

[a]These values of Ω are for demonstration purposes and should not be considered accurate. Our best estimates of Ω will be published separately (Grachev and Severinghaus, in prep.). The relative values of Ω determined from firn air are the main product of this paper.
[b]Method of Fuller et al. as given by *Reid et al.* [1977].

[9] Actual diffusivity may vary widely from the given relation, however, in response to small-scale fluctuations in density (for example, those caused by seasonal layering) that are not resolved by the Herron-Langway model [*Fabre et al.*, 2000]. For example, *Fabre et al.* [2000] found actual diffusivities that were ~70% of free-air diffusivities in near-surface firn at Queen Maud Land and De08 (Antarctica) sites, in contrast to a value of ~90–100% that would be predicted by (2). To test the sensitivity of our result to this issue, we ran the model with 30% lower diffusivity. This produced a negligible (<0.001) change in the resulting relative thermal diffusion sensitivities.

[10] The thermal diffusion sensitivity Ω is measured by equilibrating air in a known temperature gradient in the laboratory and measuring the resulting steady state isotopic fractionation [*Severinghaus and Brook*, 1999; Grachev and Severinghaus, manuscript in preparation, 2001]. It is defined empirically as the observed fractionation divided by the temperature difference. For nitrogen isotopes, for example, it is

$$\Omega^{15} \equiv \delta^{15}N/\triangle T, \quad (3)$$

where

$$\delta^{15}N \equiv [(^{15}N/^{14}N_{cold})/(^{15}N/^{14}N_{hot}) - 1]10^3‰, \quad (4)$$

$$\triangle T \equiv T_{hot} - T_{cold}. \quad (5)$$

The physical chemistry literature contains a large body of work on thermal diffusion completed over the past 83 years, most of it aimed at elucidating the intermolecular force during molecular collisions, to which thermal diffusion happens to be extraordinarily sensitive [*Grew and Ibbs*, 1952]. These works use a slightly different parameter to describe the magnitude of the thermal diffusion effect, called the "thermal diffusion factor" and denoted α or α_T and defined by the relation

$$\alpha_T \equiv \ln(R_c/R_h)/\ln(T_h/T_c), \quad (6)$$

where R_c and T_c are the isotope ratio and absolute temperature of the cold gas parcel, respectively, and R_h and T_h are the isotope ratio

Table 2. Characteristics of Firn Air-Sampling Sites

	Sites	
	South Pole	Siple Dome
Location	90°S	81°40′S, 148°46′W
Elevation, m	2841	620
Mean annual temperature,[a] °C	−51.0	−25.4
Barometric pressure, hPa	681	940
Snow accumulation, m ice eq. yr^{-1}	0.08	0.13
Firn thickness,[b] m	114	48
Date of shallow borehole drilling	Jan. 22, 1998	Dec. 9, 1996
Sampling dates (shallow holes)	Feb. 8 1998	Dec. 18, 1996
	July 28, 1998	Jan. 14, 1998
Dates of deep borehole drilling	-	Dec. 15–21, 1996
Sampling dates (deep hole)	-	Dec. 15–21, 1996 (bladder method)
	-	Jan. 14, 1998 (tube method)

[a]Temperatures from measurements made at the site at the time of sampling.

[b]Thickness of the permeable portion of the firn in which air exchanges with the atmosphere; determined from $\delta^{15}N$ data (South Pole value from *Battle et al.* [1996]).

and absolute temperature of the hot gas parcel. For convenience, we use Ω rather than α_T because α_T is strongly dependent on absolute temperature, while Ω is nearly independent of temperature in the temperature range of polar firn. To convert α_T to Ω, one may use the relation (Grachev and Severinghaus, manuscript in preparation, 2001)

$$\Omega \cong \frac{\alpha_T}{T_{\text{average}}} 10^3‰\ \text{K}^{-1}, \tag{7}$$

where

$$T_{\text{average}} \equiv \frac{T_h T_c}{T_h - T_c} \ln \frac{T_h}{T_c}. \tag{8}$$

[11] The firn heat model is adapted from *Alley and Koci* [1990] and is forced at the top boundary (i.e., the surface) with the observed temperature history (Figure 1). The bottom boundary of the model (the firn-ice transition) is impermeable to gas and insulating to heat. Although clearly inadequate for longer integrations, the insulating boundary condition is adequate for our 10-year runs. The temperature predicted by the heat model is used as input to the gas model at each time step. The heat model is initialized with the mean annual temperatures, with an isothermal column (South Pole) or a geotherm of 0.01°C m^{-1} (Siple Dome). The model is run for 10 years before the sampling date to insure that no "memory" of the initial condition remains (other than the geotherm, which does persist). The model has boxes 0.5 m in the vertical with a time step of 1 hour.

[12] Comparison of the modeled temperature profiles with several measurements (taken from thermistors buried in the boreholes) shows good agreement for Siple Dome in 1996 (Figure 2a). Agreement is also good for the South Pole (Figure 5a). For the South Pole, Automatic Weather Station temperature data 0.5 m above the surface from the "clean air" station were used as the model forcing from 1996 onward (Figure 1). Before that, an idealized temperature history was used that represents approximately a stacked average of 10 years of South Pole temperature data. However, the result is quite insensitive to the temperature history beyond a year or so. At Siple Dome the Automatic Weather Station (AWS) did not exist prior to 1997, so an

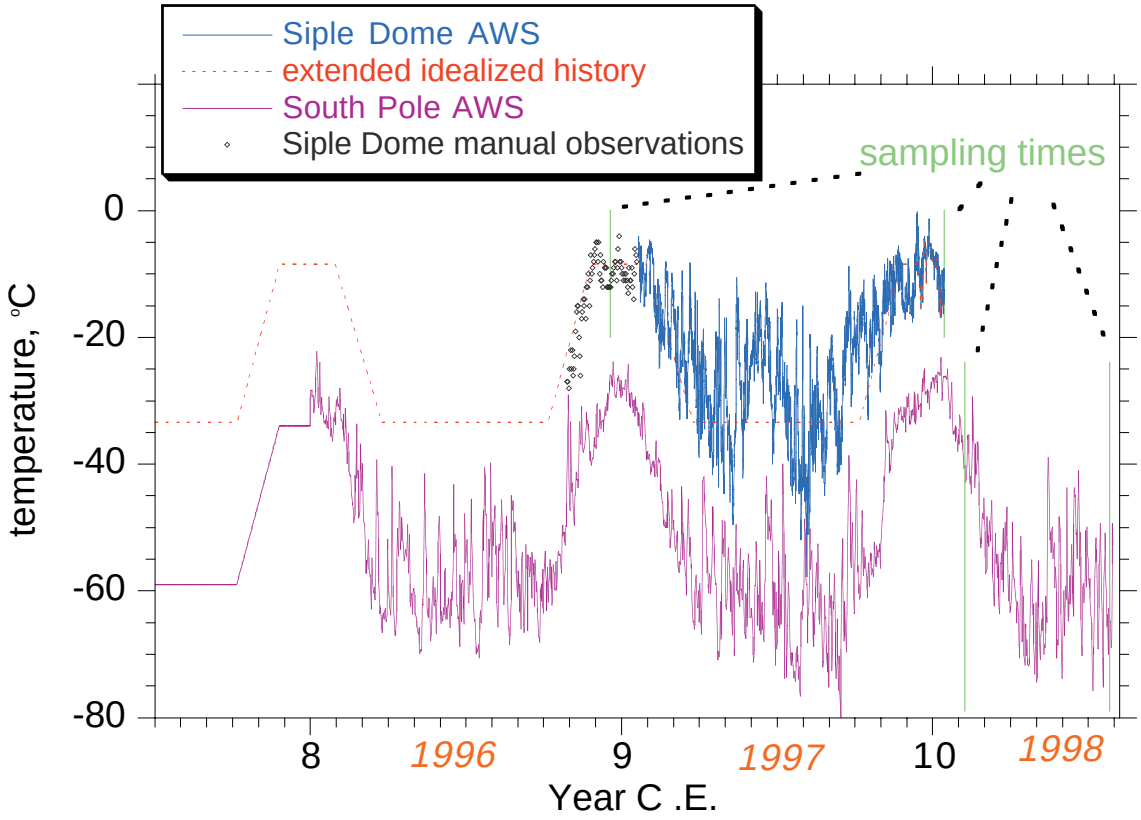

Figure 1. Surface temperature histories used as the model forcing at the upper boundary condition. Automatic Weather Station (AWS) data are used where possible. Idealized histories are used where no AWS data are available or before the range of thermal memory. AWS data at Siple Dome (top plot) seem to be in conflict with the measured 1998 firn temperature profile, leading us to use the alternative "extended idealized history" (dashed line) (see text).

idealized record was used that was constructed by adding 25.5°C to the South Pole idealized history (the amount required to give the mean annual temperature correctly). The Siple Dome AWS data for 0.5 m were not available, so data from 3 m above surface were used. Unfortunately, no snow surface temperature data were available at either location, which would have been desirable because near-surface inversions are common on polar ice sheets [*Connolley*, 1996].

[13] The agreement of the 1998 Siple Dome modeled temperature profile with the observed temperatures is rather poor when forced with the AWS data (Figure 2b). The reason for this is not clear. Sensitivity tests varying the thermal conductivity of the firn by 50% did not improve the fit. Somewhat arbitrarily, we forced the model with an extended idealized history that was replaced with the AWS data for only the last 32 days of the simulation (Figure 1). This resulted in a much better fit to the temperature observations (Figure 2b). Either the model badly misrepresents the thermal conductivity structure of the firn (which is a function of firn density in the model) or the AWS data does not represent surface temperature. The primary disagreement between the two histories is in the timing of the spring warming in October–

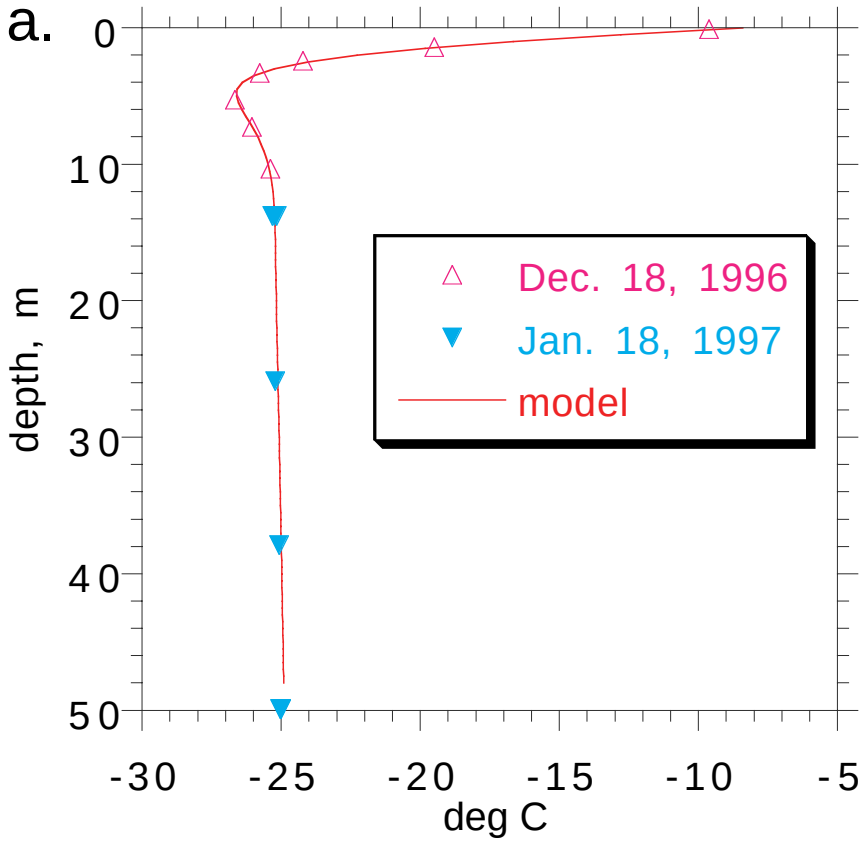

Figure 2. Depth profiles of measured temperature at Siple Dome in (a) 1996 and (b) 1998. Thermistors were placed in the borehole and measured at the surface with a Newport INFCH Thermistor digital panel readout. Thermistors were calibrated in a chilled ethanol bath with a precision mercury thermometer and were accurate to better than 0.1°C.

November 1997 (Figure 1). At present we cannot resolve this conflict, so we present both scenarios, noting that the impact on our calculated relative thermal diffusion sensitivities is negligible.

3. Sampling and Analysis

[14] Samples of firn air were withdrawn in two different ways. The first method (the "bladder method") involved drilling down to the desired sampling depth and inserting an inflatable rubber bladder to seal off the sampling horizon from atmospheric contamination [*Schwander et al.*, 1993; *Bender et al.*, 1994a; *Battle et al.*, 1996]. Gases were then pumped from the bottom of the bladder though tubes and into 2-L glass flasks. The second method is experimental and was developed specifically for shallow firn air recovery (the "tube method"). Eight polyethylene-aluminum composite (Dekaron) tubes of varying lengths with stainless steel screens affixed to the ends were placed in an open, freshly drilled borehole. The hole was backfilled with snow and layers of slush to impede vertical movement of air. After backfilling, the tubes were pumped on to remove as much contamination as possible. Sampling by pumping on the tubes was done after waiting 1–2 weeks (or years in some cases) for any

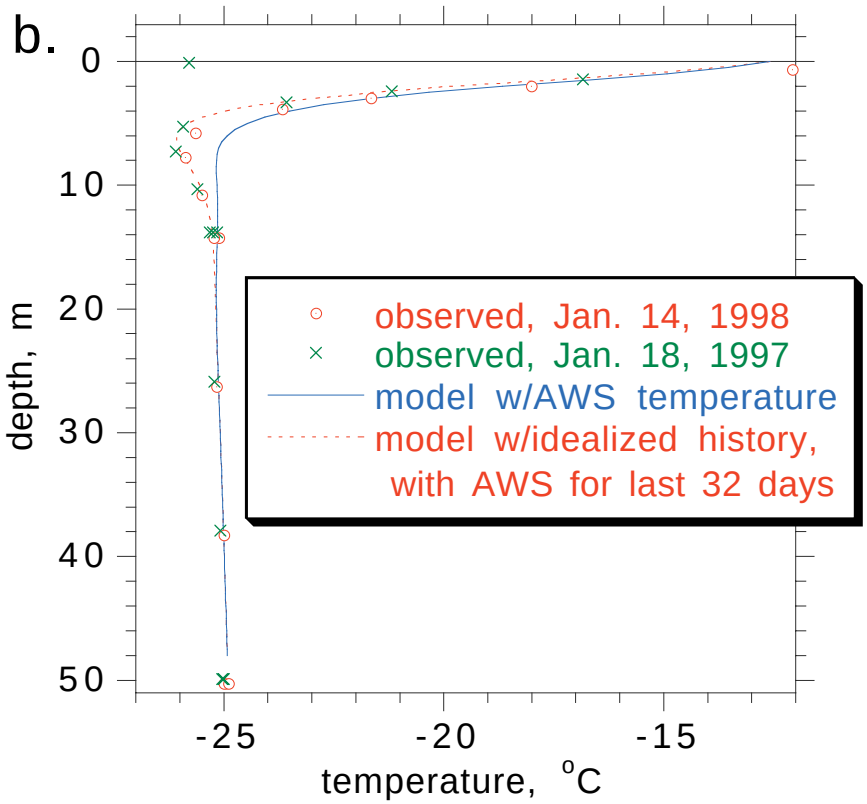

Figure 2. (continued)

residual contamination to disperse. This technique is similar to that used to sample air in sand dunes [*Severinghaus et al.*, 1997].

[15] The tube method takes advantage of the fact that the strong horizontal layering of the firn gives it a relatively high horizontal permeability compared to its vertical permeability [*Albert et al.*, 2000], so that air is less likely to be sucked down from higher levels during sampling than in an isotropic medium. Where possible, the backfill was compacted with a long rod to reduce vertical permeability along the borehole. To the same end, small amounts of slush (snow mixed with water melted on site with an electric heater) were used as the backfill in between the intake screens. The slush quickly froze and formed "ice plugs," which are thought to be relatively impermeable. Sampling was done in sequence, from shallowest to deepest, to minimize the possibility that air from shallower depths had been drawn down into an intake screen.

[16] At South Pole the tubes in the hole were extended along the surface and into the National Oceanic and Atmospheric Administration (NOAA) Clean Air Building to enable indoor sampling during winter. The borehole was located 42 m due grid E of the NE corner of the Clean Air Building (grid N is in the direction of Greenwich). At Siple Dome, two holes 46 m apart were drilled, one 15 m deep (the "shallow hole") and one 92 m deep (the "C Core hole"). An ice core (the Siple Dome C Core) was recovered from the latter hole during firn air sampling via the bladder method. After completion of the C Core hole, six tubes were

installed in the hole at depths from 16 to 56 m as a test of the tube method in the deep firn, and the hole was backfilled with sand and snow. These tubes were sampled 1 year later.

[17] Samples were pumped at 4 L min^{-1} for 16 min to flush the lines and the sample flasks. In both methods (bladder and tube) the air was dried by passing it through a column packed with granular phosphorous pentoxide. The air was stored in 2-L flow-through glass flasks as described by *Battle et al.* [1996]. Flasks were analyzed mass spectrometrically at the University of Rhode Island (URI) and Scripps Institution of Oceanography (SIO) for $^{15}N/^{14}N$ and $^{40}Ar/^{36}Ar$ ratios and other gas ratios, including $^{40}Ar/^{38}Ar$, $^{18}O/^{16}O$ of O_2, O_2/N_2, $^{84}Kr/^{36}Ar$, and $^{132}Xe/^{36}Ar$. Techniques for the analysis of $^{15}N/^{14}N$, $^{18}O/^{16}O$ of O_2, and O_2/N_2 in Siple Dome samples were as given by *Bender et al.* [1994b]. For these gases in South Pole samples, flask air was expanded into a 0.8 cm^3 evacuated stainless steel volume, the volume was closed, and this aliquot was in turn expanded into the mass spectrometer and run following the technique of *Sowers et al.* [1989]. Small corrections were made to all data according to standard procedure [*Bender et al.*, 1994b] to account for CO^+ isobaric interference and the sensitivity of the mass spectrometer's measured $\delta^{18}O$ to variation in $\delta N_2/O_2$ (the so-called "chemical slope") [*Bender et al.*, 1994b]. A small further correction to the URI $^{18}O/^{16}O$ data appeared to be required after rerunning a subset of the samples on the SIO mass spectrometer, whose chemical slope is a factor of ~22 smaller than that of URI. The SIO results were then used to adjust the chemical slope applied to the original URI data set in such a way as to minimize the squared mismatch between the overlapping sets.

[18] Noble gases were analyzed by exposing 40 standard cm^3 of air sample to a Zr/Al getter at 900°C for 10 min to destroy all reactive gases. The oven temperature was then lowered to 300°C for 2 min to absorb H_2. Residual gases were frozen quantitatively into a stainless steel container at 4 K, then warmed to room temperature and admitted to the mass spectrometer after sitting for 45 min to allow homogenization. Dual-collector measurements were made of $\delta^{40}Ar$ ($^{40}Ar/^{36}Ar$) and $\delta^{38}Ar$ ($^{40}Ar/^{38}Ar$) on a dynamic-inlet Finnegan MAT 252 isotope ratio mass spectrometer, and $\delta^{84}Kr$ ($^{84}Kr/^{36}Ar$) and $\delta^{132}Xe$($^{132}Xe/^{36}Ar$) were measured in a single collector by periodically varying the magnetic field ("peak jumping").

[19] One measurement, of $\delta^{132}Xe$ from 30.55 m depth at Siple Dome in 1996, was rejected on the basis of poor agreement with replicate aliquots. Results of two aliquots, measured for $\delta^{15}N$, $\delta^{18}O$, and $\delta O_2/N_2$ from 3 m depth at South Pole on February 8, were rejected on the basis of high CO_2 concentrations (22 and 31% above normal) that suggested gross contamination with laboratory air.

[20] For the remaining samples taken in 1998, the pooled standard deviation s_{pooled} of flask pairs from the same depth was 0.005‰ for $\delta^{15}N$, 0.010‰ for $\delta^{18}O$, 0.029‰ for $\delta O_2/N_2$, 0.009‰ for $\delta^{40}Ar$, 0.009‰ for $\delta^{38}Ar$, 0.09‰ for $\delta^{84}Kr$, and 0.25‰ for $\delta^{132}Xe$. In 1996 Siple Dome shallow samples, there appears to be a bias (~0.02–0.03‰ in $\delta^{15}N$) based on the deviation of the surface samples from the expected value of zero, and reproducibility is worse than expected in both shallow and deep 1996 samples (s_{pooled} = 0.006‰ for $\delta^{15}N$ versus 0.003 expected value). We believe that this bias is probably due to artifactual thermal fractionation during sampling. During flask flushing at Siple Dome in 1996, the flasks were heated on one side in order to keep the elastomer o-rings from freezing, and in retrospect, it seems likely that this heating caused thermal convection inside the flasks. A thin layer of rising warm air at the wall of the flask

is bounded by a cooler sinking region in the flask interior, and thermal fractionation occurs horizontally across this temperature gradient. The result is a progressive depletion of the heavy isotope in the rising air, the phenomenon exploited in the Clusius-Dickel thermal diffusion column that was used to separate uranium isotopes during the 1940s [*Grew and Ibbs*, 1952]. Because the flasks were oriented with the exit port at the top, any fractionated warm air would have preferentially left the flask, causing a bias in the remaining air. This artifact was the primary motivation for returning to Siple Dome in 1998. The problem was addressed in 1998 by keeping the flasks isothermal during flushing. We also chose to orient the flask horizontally, with the exit port midway between the upper and lower walls of the flask. Consequently, warm fractionated air that rose to the top of the flask would not have a greater or lesser chance of leaving the flask than cool air. These protocol changes appear to have solved the problem. For the purpose of calculating relative thermal diffusion sensitivities, we subtracted from all Siple Dome δ^{132}Xe/96 values the mean deviation of the surface air samples from zero, -0.0046‰ in 1996 data and -0.0097‰ in 1998 data. The surface air samples should have been zero, and we assume that the bias (whatever the cause) affected all downhole data equally.

4. Results

4.1. Siple Dome

[21] Gravitational settling enriches the heavier molecules at the bottom of a stagnant air column in proportion to the mass difference Δm, so gravity should affect δ^{40}Ar almost exactly 4 times as much as δ^{15}N [*Gibbs*, 1928; *Lindemann and Aston*, 1919; *Craig et al.*, 1988; *Sowers et al.*, 1989; *Schwander*, 1989]. Thus, if gravity were the only process acting on a gas mixture, δ^{15}N would be equal to δ^{40}Ar/4 at all depths. To facilitate comparison, all results are presented here with the δ value divided by Δm. Siple Dome firn air profiles taken in 1996 and 1998 show the expected downward linear increase in δ^{15}N and δ^{40}Ar/4 due to gravitational settling (Figures 3a and 3b). Superimposed on this increase is a bell-shaped heavy-isotope anomaly in the top $\sim$10 m that we hypothesize is the result of thermal diffusion acting in response to the sharp seasonal temperature gradient near the surface. This anomaly resembles the one seen in air drawn from a sand dune [*Severinghaus et al.*, 1996]. Because gases diffuse $\sim$10 times faster than heat in firn [*Paterson*, 1969], the isotopic anomaly extends deeper than the temperature anomaly. The upper and lower limbs of this anomaly are conceptually distinct: the upper limb is in quasi-equilibrium with the temperature gradient (Figure 2b), with heavier isotopes occupying colder regions. The lower limb, in contrast, is a transient wave that is propagating downward into nearly isothermal firn and can be thought of as a mixing line between air of two different compositions.

[22] The model overestimates the thermal fractionation anomaly seen in the data in 1996 but comes close to matching its amplitude, if not its shape, in 1998 (Figure 3). As discussed above, the AWS-forced model does a poor job of predicting the observed 1998 temperature profile, so it is not surprising that it also does a poor job of predicting the transient part of the isotope profile. The extended idealized history comes much closer to fitting both the temperature and isotopic data. Despite sampling artifacts, the mismatched shape in 1996 is harder to understand because the model fits the temperature data quite well. One possible explanation is that wind pumping [*Colbeck*, 1989] may have convectively ventilated the firn shortly before sampling, thus reducing the amplitude of the anomaly. The amplitude of the thermal diffusion anomaly is decreased by

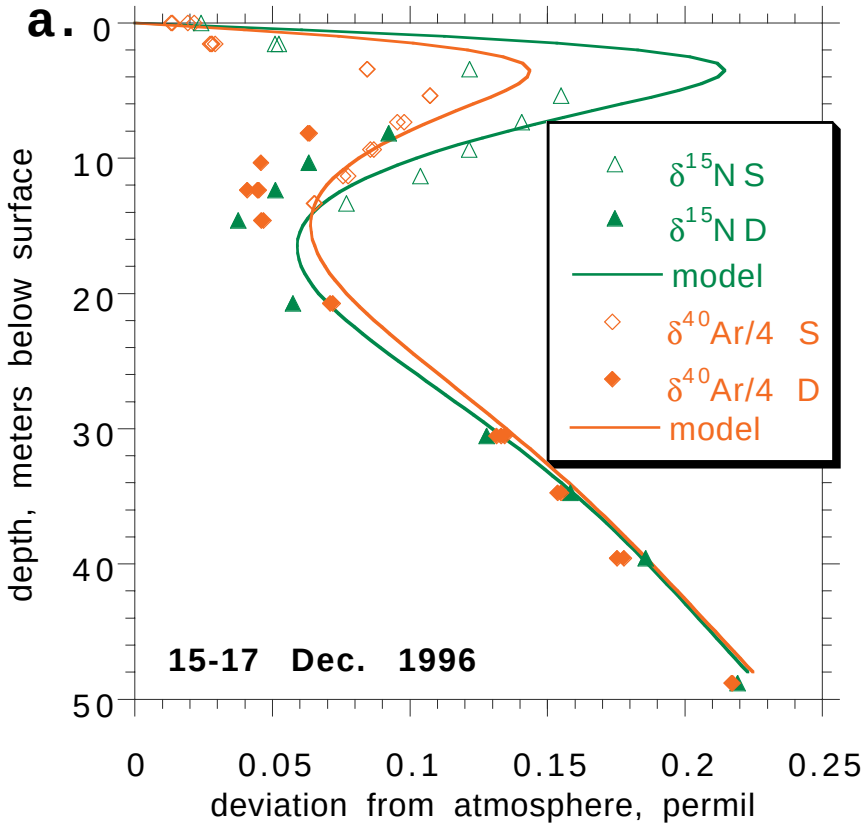

Figure 3. Argon and nitrogen isotope ratios versus depth in the firn at Siple Dome in (a) December 1996 and (b) January 1998. "Deep" (D) samples in 1996 were sampled by the "bladder method," and "shallow" (S) samples were sampled by the "tube method" (see text). The curves are pure diffusion model results with no adjustable parameters. The rough fit (to within 30%) of model and data supports the hypothesis that thermal diffusion is responsible for the near-surface bell-shaped anomaly but does not permit a precise quantification of the coefficients of thermal diffusion. Note that argon is less sensitive to thermal diffusion than nitrogen on a per mass unit difference basis, which permits the separation of gravitational and thermal effects in ice core gas isotope records.

convection because the upper few meters of the firn column are effectively like the atmosphere (well-mixed), so that the temperature gradient in that interval has no isotopic effect. Only the temperature gradient existing in the region below the convective zone will be expressed in the isotopes. Leaving 1996 aside, the good match of the model to the quasi-equilibrium part of the 1998 anomaly suggests to first order that our laboratory estimates of Ω are not far off and that thermal diffusion in snow is not very different from thermal diffusion in the laboratory.

[23] All measured gases at Siple Dome are shown in an expanded view of the top 22 m in Figures 4a and 4b. The 1996 model results have an arbitrary "convective zone" added, and 1998 model results are driven by the extended idealized history (Figure 1). As expected from literature values of α_T, the thermal diffusion sensitivities of δ^{84}Kr/48 and δ^{132}Xe/96 appear

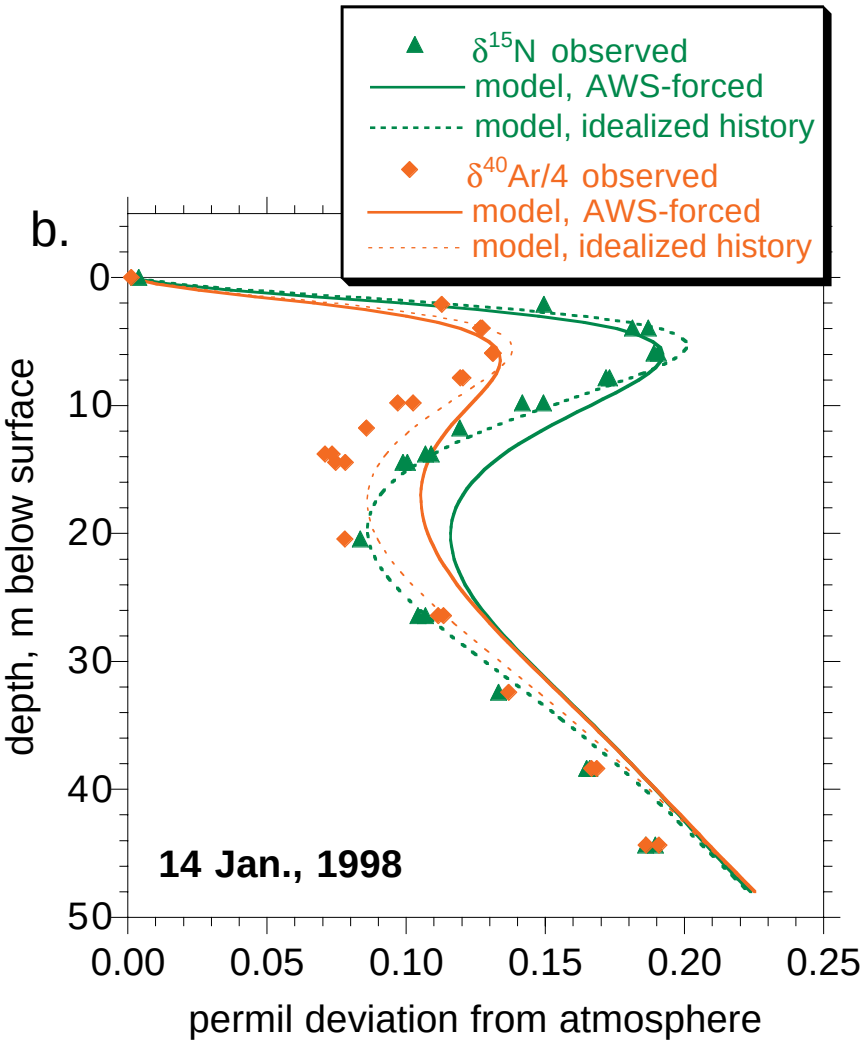

Figure 3. (continued)

much weaker than that of $\delta^{15}N$, with small anomalies observed in the data. These gas pairs are mostly affected by gravity and would make excellent indicators of gravitational settling in ice core records were it not for molecular size-dependent fractionation processes during bubble enclosure [*Severinghaus and Brook*, 2000]. Both $\delta^{18}O/2$ and $\delta O_2/N_2/4$ are slightly less sensitive to thermal diffusion than $\delta^{15}N$, as seen in our laboratory experiments (Grachev and Severinghaus, manuscript in preparation, 2001). Measured $\delta^{38}Ar/2$ is indistinguishable from $\delta^{40}Ar/4$ and does not add much scientific value to $\delta^{40}Ar/4$ because of its lower precision.

[24] Small differences exist between some shallow and deep hole data in depth intervals where the two data sets overlap (Figures 4a and 4b). One possibility is that sampling of the shallow hole via the tube method drew air down from shallower levels into the intake screens. This seems unlikely because if this were true, flasks drawn later should exhibit

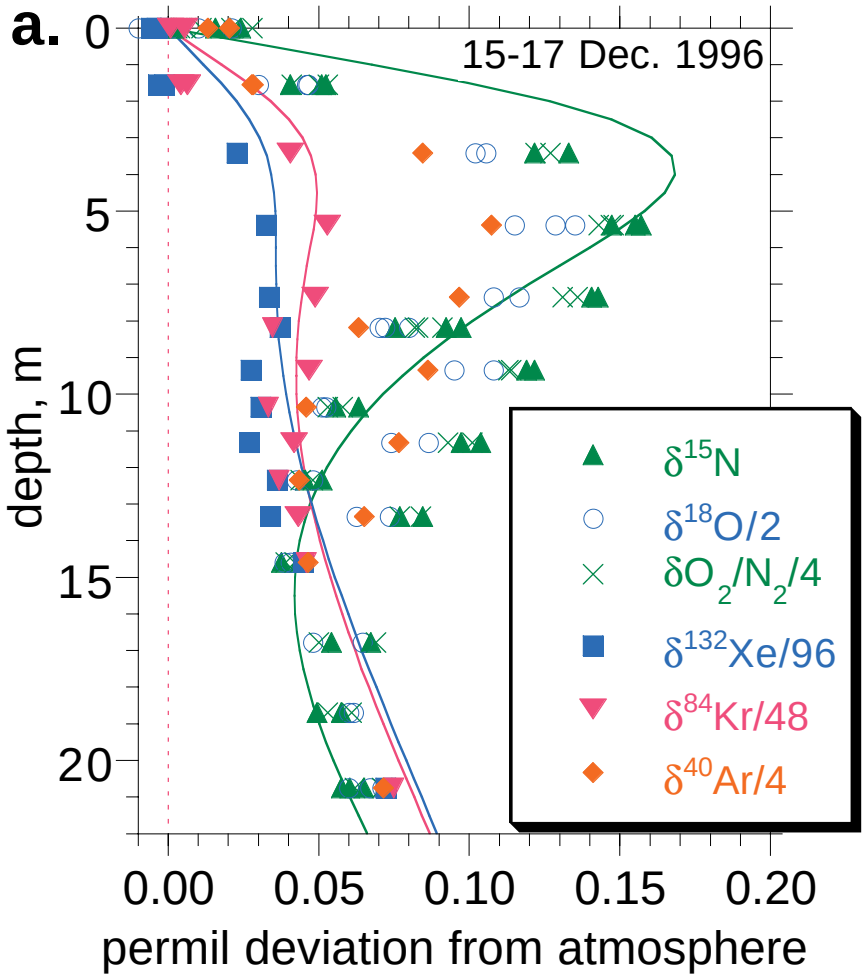

Figure 4. Expanded view of Siple Dome thermal diffusion anomaly in the top 20 m of the firn, showing all measured gases. (a) Data from 1996, which are poorly modeled using only diffusion. Note the two distinct sets of data collected from two separate holes (see text). Model $\delta^{15}N$ results shown for 1996 were generated with an arbitrary "convective zone" introduced into the model by including an eddy diffusion term as a second term on the right-hand side of equation (1). The eddy diffusivity is 6×10^{-5} m^2 s^{-1} at the surface and falls off exponentially with depth with a scale height of 1.5 m, which is the general form expected of windpumping [*Colbeck*, 1989]. (b) Data taken in 1998, with improvements in sampling protocol to eliminate artifacts (see text). Model curves shown are diffusion-only runs forced by the extended idealized history. The $\delta^{18}O/2$ curve is obtained by scaling $\delta^{15}N$ by 0.83, the relative thermal diffusion sensitivity calculated below.

more bias than flasks drawn earlier in the sampling. No such dependence on sampling order was observed, and successively sampled flask values were highly constant (s_{pooled} = 0.003‰ for $\delta^{15}N$ in Siple Dome 1998 samples). As a test of the durability of the firn as an air archive, repeat flasks were taken at two depths, 1.55 m and 5.39 m, after flushing ~110 L over a 50 min period. These repeat flasks showed no change from flasks taken at the beginning of the flushing ($\delta^{15}N$ of the repeat flask was 0.051‰ versus 0.046‰ at

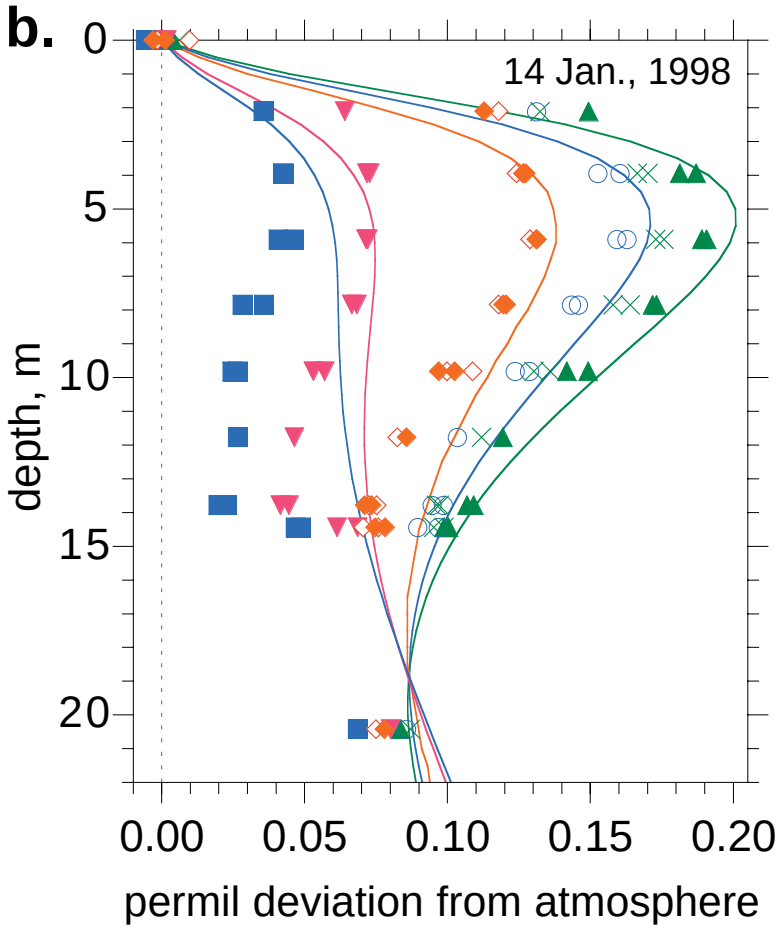

Figure 4. (continued)

the start, 1.55 m; $\delta^{15}N$ of the repeat flask was 0.147‰ versus 0.156‰ at the start, 5.39 m). Thus the small differences between shallow and deep data remain unexplained.

4.2. South Pole

[25] Winter firn air profiles have the potential to place constraints on the possible role of thermally driven (Bernard) convection in the firn. In winter the temperature gradient is reversed from the more commonly studied summer profile (Figure 5a). Cold dense air overlies warmer air in the firn and might become unstable and undergo Bernard convection [*Powers et al.*, 1985]. If the wintertime thermal diffusion anomaly were not expressed because of convection, but the summer one were, the annual mean thermal fractionation signal would be nonzero even when annual mean temperature change was zero. In other words, there would be a rectifier of seasonal temperature change, and this signal would be transmitted to the deep firn, creating a bias in the bubble air-based thermal diffusion paleoindicator.

[26] The tendency to undergo Bernard convection in a porous media can be estimated from the dimensionless Rayleigh number, with the

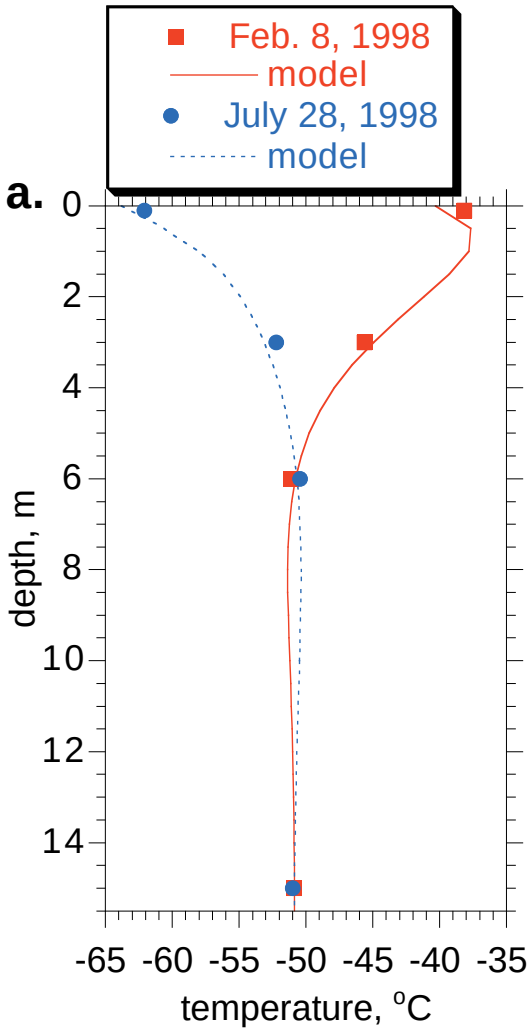

Figure 5. South Pole records of (a) shallow firn temperature, (b) winter gas data, and (c) summer gas data. Model curves are driven by measured surface temperatures very close to the site (Clean Air AWS). Note the good fit of the model to the temperature profile observations and the near-symmetry of the seasonally opposite temperature profiles.

slight modification that the thermal diffusivity is the ratio of the thermal conductivity of snow to the volumetric heat capacity of air [*Powers et al.*, 1985]. Taking the coefficient of thermal expansion of air as 0.0045 K^{-1}, the depth of the layer with strong temperature gradient as 5 m, the temperature difference across this layer as 10 K, the permeability of the firn as 4×10^{-9} m^2, the dynamic viscosity of air as 1.4×10^{-5} kg m^{-1} s^{-1}, and the thermal diffusivity as 0.22 m^2 s^{-1}, a Rayleigh number of 4 is obtained. This is sufficiently close to the critical value for the onset of convection (10–30) that natural convection in snow cannot be ruled out by this calculation. Further, our calculation assumes a one-dimensional firn and ignores other time-dependent processes that might initiate convection. For example, wind pumping

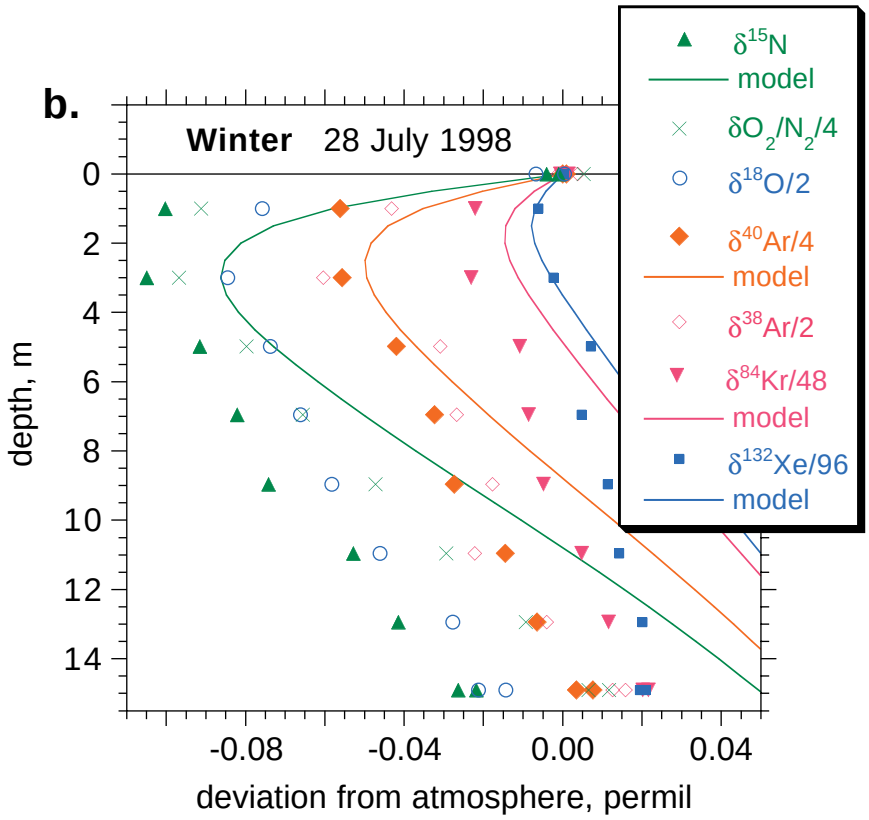

Figure 5. (continued)

beneath topographic roughness (snow dunes or sastrugi) might get convection started [*Colbeck*, 1989]. Polar ice core sites are sufficiently horizontal that downslope gravity flow is much slower than the rate of transport by molecular diffusion (~1 m^2 d^{-1}), and thus downslope flow can be neglected.

[27] If vigorous convective stirring during winter were important, we would expect to see a greatly attenuated thermal fractionation signal. In fact, we observed a fully developed negative isotope anomaly, with an amplitude slightly larger than that predicted by the pure diffusion model driven by observed surface air temperature (Figure 5b). The same tube array sampled in summer is shown for comparison in Figure 5c. The summer data fit the model well and generally confirm the relative values of Ω derived at Siple Dome. The winter data deviate markedly from the deeper part of the model, which we do not understand. As discussed below, these data also yield relative thermal sensitivities inconsistent with sensitivities derived from the other collections. It seems possible that gradual downward flow is advecting the values obtained at shallower depths to deeper levels. Alternatively, intermittent turbulent convective mixing may be weak enough that it does not homogenize and erase the isotope fractionation yet strong enough that it acts to transport the isotope signal downward into the firn faster than would molecular diffusion alone. In other words, mixing by eddy diffusion would double or triple the effective diffusivity over the molecular diffusivity. Adding an arbitrary intermittent eddy diffusion term to

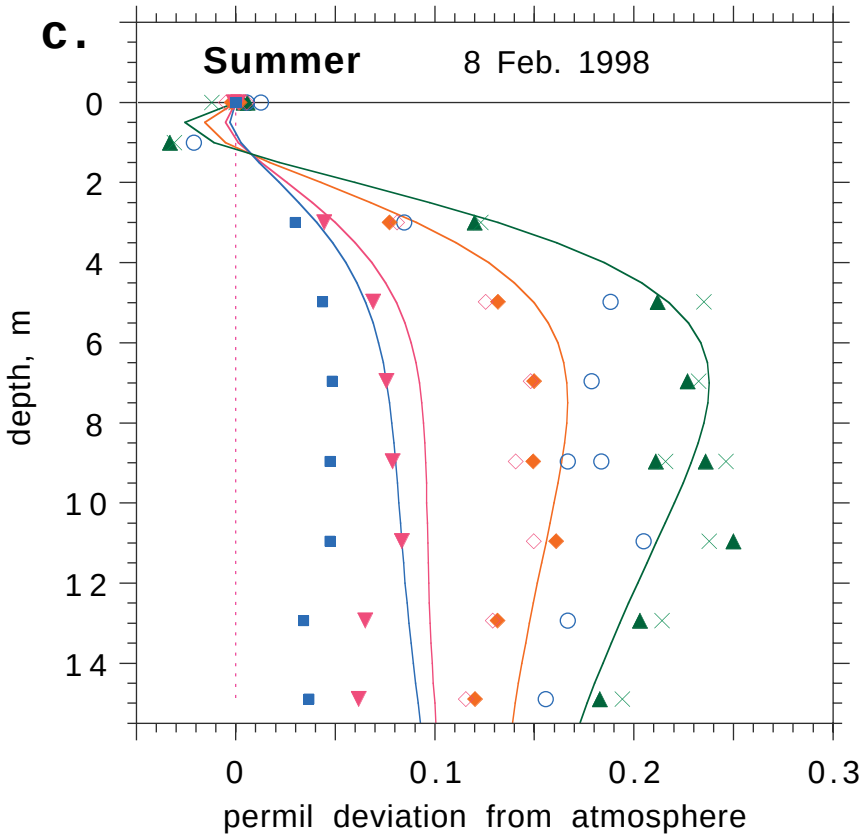

Figure 5. (continued)

our model produces this effect, demonstrating plausibility but not proof.

5. Relative Thermal Diffusion Sensitivities

[28] The uncertainty of the model and its temperature history prohibit a precise estimate of the absolute thermal diffusion sensitivities from our field data. However, the relative thermal diffusion sensitivities of different gas pairs may be calculated with confidence, because all gases share the same temperature history and diffusion path. The relative sensitivity Ω^{40}/Ω^{15} of argon and nitrogen isotopes is of particular interest because their difference in sensitivity is used to calculate the magnitude of temperature change in ice core records from observed $\delta^{15}N$ and $\delta^{40}Ar/4$ [*Severinghaus and Brook*, 1999]. When combined with the laboratory-determined value of Ω^{15}, this relative sensitivity can yield an improved estimate of the difference $\Omega^{15} - \Omega^{40}/4$.

[29] In order to calculate relative values of Ω from the data, the effect of gravitational settling δ_{grav} must first be removed. We do this by taking advantage of the fact that Xe/Ar is dominated by gravitational settling, so error in estimating the gravitational component of $\delta^{132}Xe$ is small. The small thermal diffusion signal in $\delta^{132}Xe$ is removed using observed $\delta^{15}N$ and our laboratory measurements of Ω^{15} and Ω^{132} (Table 3). Circularity introduced by this correction is negligible owing to the small value of Ω^{132}. We must also account for the fact that all gases diffuse at slightly different speeds, and the gases

Table 3 (Representative Sample). Calculation of Relative Thermal Diffusion Sensitivities [The full Table 3 is available in ASCII tab-delimited format at http://g-cubed.org.]

		Measurement Error[a]					
Flask ID	Depth, m	0.005 $\delta^{15}N$	0.005 $\delta^{18}O/2$	0.007 $\delta O2/N2/4$	0.002 $\delta^{40}Ar/4$	0.002 $\delta^{84}Kr/48$	0.003 $\delta^{132}Xe/96$
			Siple Dome Dec. 18, 1996				
sdf03	1.55	0.0524	0.0459	0.0499	0.0279	0.0042	−0.0363
sdf05	1.55	0.0509	0.0465	0.0534	0.0283	0.0064	−0.0341
sdf06	3.42	0.1216	0.1057	0.1222	0.0845	0.0405	0.0000
sdf08	5.39	0.1550	0.1283	0.1467	0.1073	0.0529	0.0124
sdf11	7.35	0.1407	0.1078	0.1307	0.0967	0.0488	0.0083
sdf13	9.35	0.1216	0.1082	0.1137	0.0863	0.0468	0.0063
sdf15	11.32	0.1038	0.0864	0.1006	0.0766	0.0418	0.0013
Error-weighted mean							
Error-weighted rms deviation							
			Siple Dome Jan. 14, 1998				
158	2.11	0.1494	0.1310	0.1324	0.1128	0.0641	−0.0086
62	3.95	0.1813	0.1602	0.1664	0.1268	0.0718	−0.0009
521	3.95	0.1870	0.1525	0.1701	0.1274	0.0727	0.0000
289	5.90	0.1907	0.1591	0.1729	0.1313	0.0716	−0.0011
520	5.90	0.1891	0.1627	0.1757	0.1310	0.0721	−0.0006
350	7.84	0.1731	0.1457	0.1580	0.1204	0.0665	−0.0062
130	7.84	0.1718	0.1433	0.1640	0.1194	0.0683	−0.0044
349	9.82	0.1418	0.1236	0.1303	0.0970	0.0530	−0.0197
141	9.82	0.1493	0.1286	0.1359	0.1026	0.0570	−0.0157
302	11.77	0.1193	0.1033	0.1119	0.0857	0.0464	−0.0263
28	13.78	0.1091	0.0984	0.0962	0.0735	0.0445	−0.0282
195	13.78	0.1069	0.0945	0.0971	0.0710	0.0415	−0.0312
Error-weighted mean							
Error-weighted rms deviation							
Total Siple Dome							

[a]Pooled standard deviation of replicate flasks; 1 sigma.

are not quite at equilibrium with the temperature. This disequilibrium effect ε is estimated by running the model with the nitrogen diffusivity D^{15} assigned to the other gas, denoted gas x. The result is then subtracted from the ordinary result δ^x, giving

$$\varepsilon^x \equiv \delta^x_{\text{model}} - \delta^x[D^{15}]_{\text{model}} \quad \varepsilon^{15} \equiv 0 \tag{9}$$

A separate ε^x value is calculated for each depth, and they are smaller than ±0.008‰ in all cases. To calculate δ_{grav}, we note that observed values $\delta^{15}N_{\text{obs}}$ are a combination of gravitational effect $\delta^{15}N_{\text{grav}}$, thermal effect $\delta^{15}N_{\text{therm}}$, and disequilibrium effect ε^{15}:

$$\delta^{15}N_{\text{obs}} = \delta^{15}N_{\text{grav}} + \delta^{15}N_{\text{therm}} + \varepsilon^{15} \tag{10}$$

$$\delta^{132}Xe_{\text{obs}} = \delta^{132}Xe_{\text{grav}} + \delta^{132}Xe_{\text{therm}} + \varepsilon^{132}. \tag{11}$$

It should be noted that $\delta^{132}Xe_{\text{grav}}$ and $\delta^{132}Xe_{\text{therm}}$ are the values that would be observed if Xe had the diffusivity D^{15}. Taking advantage of the facts that $\delta^{132}Xe_{\text{grav}}/\Delta m = \delta^{15}N_{\text{grav}} = \delta_{\text{grav}}$ and that $\delta^{15}N_{\text{therm}} = \Omega^{15}\Delta T\gamma$, where γ is an arbitrary disequilibrium term, these two equations may be written as

$$\delta^{15}N_{\text{obs}} = \delta_{\text{grav}} + \Omega^{15}\triangle T\gamma \tag{12}$$

$$\frac{\delta^{132}Xe_{\text{obs}}}{\triangle m} = \delta_{\text{grav}} + \frac{\Omega^{132}}{\triangle m}\triangle T\gamma + \frac{\varepsilon^{132}}{\triangle m}. \tag{13}$$

For brevity, we will not write Δm henceforth, but all δ, Ω, and ε will be implicitly divided by Δm unless specified otherwise. Multiplying (12) by Ω^{132} and (13) by Ω^{15} and solving for δ_{grav}, we have

$$\delta_{\text{grav}} = \frac{\delta^{132}Xe_{\text{obs}} - \varepsilon^{132} - \frac{\Omega^{132}}{\Omega^{15}}\delta^{15}N_{\text{obs}}}{\left(1 - \frac{\Omega^{132}}{\Omega^{15}}\right)}. \tag{14}$$

Treating Ω^{15} as an unknown now, the ratios of the thermal diffusion sensitivities are calculated (excepting Ω^{132} to avoid circularity) via the following:

$$\frac{\Omega^x}{\Omega^{15}} = \frac{\delta^x - \varepsilon^x - \delta_{\text{grav}}}{\delta^{15}N_{\text{obs}} - \delta_{\text{grav}}}. \tag{15}$$

Measurement errors of the five observed quantities (δ^x_{obs}, $\delta^{15}N_{\text{obs}}$, $\delta^{132}Xe_{\text{obs}}$, Ω^{15}, and Ω^{132}) are propagated assuming they are independent and normally distributed using a Monte Carlo simulation (Table 3). No error was assigned to ε, but a sensitivity test with a 50% drop in ε produced a negligible change in the ratio (+0.005). The results show fairly constant ratios in the depth intervals in which the thermal signal is strong at Siple Dome and summer South Pole, giving confidence in the result, as the ratio is expected to be a physical constant (Figure 6). The winter South Pole data set shows a systematic trend toward smaller ratios with depth, which we do not understand. It seems possible that this is related in some way to the poor fit of the data with the model (Figure 5b); perhaps both problems result from air being drawn down from higher levels during the sampling and mixed with other air parcels. Excluding the winter data, we weight each value by the inverse square of its error to calculate a site mean, finding $\Omega^{40}/\Omega^{15} = 0.659$ for Siple Dome (effective temperature T_{average} −18°C) and 0.642 for South Pole (T_{average} −43°C). In the absence of systematic error the weighted standard errors would be ±0.008 for Siple Dome and ±0.005 for South Pole, but we are unsure if systematic error can be ruled out, so we adopt an error of ±0.02 (1σ) for both sites. Similar procedures are followed for Ω^{18}/Ω^{15} and Ω^{84}/Ω^{15} (Tables 1 and 3).

[30] As an independent check of the method, we repeated the calculation using $\delta^{84}Kr_{\text{obs}}$ instead of $\delta^{132}Xe_{\text{obs}}$ to estimate δ_{grav}. The resulting Ω^{40}/Ω^{15} was 0.651 for Siple Dome and 0.615 for summer South Pole. We expect Kr to give a less accurate estimate of δ_{grav} because it is more sensitive to thermal diffusion and Ω^{84} is poorly known. Nonetheless, this check suggests that the answer is fairly insensitive to error in δ_{grav}.

[31] The small difference in Ω^{40}/Ω^{15} values for Siple Dome and South Pole is not necessarily error, as Ω varies slightly from gas pair to gas

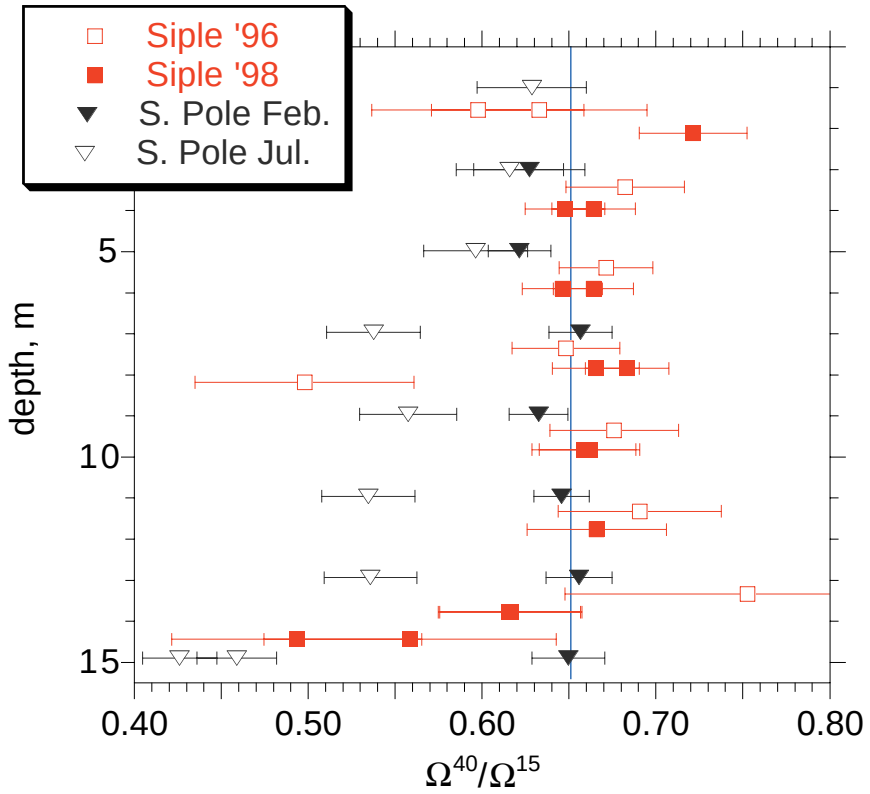

Figure 6. Calculated Ω^{40}/Ω^{15} versus depth at both Siple Dome and South Pole. Values scatter widely at the top and bottom of the profiles, but in the middle, where the signals are large, the means appear to converge on a value of 0.65 (marked by the vertical blue line).

pair in its temperature dependence. These values of Ω^{40}/Ω^{15} compare well with results of a preliminary laboratory experiment in which air was equilibrated in a known temperature gradient and the resulting isotope separation measured, giving $\Omega^{40}/\Omega^{15} = 0.647$ (Grachev and Severinghaus, manuscript in preparation, 2001). It is considerably smaller than the value obtained from a theoretical calculation based on the Lennard-Jones model [*Leuenberger et al.*, 2000]. The discrepancy may be related to the fact that the Lennard-Jones model does not account for the other gases present in air. In air, virtually all collisions involving argon molecules are with N_2 or O_2 molecules rather than other Ar molecules, and the strength of the thermal diffusion effect is dependent on the nature of the collision [*Grew and Ibbs*, 1952]. In fact, in experiments in pure Ar we obtained values of Ω^{40} that yield $\Omega^{40}/\Omega^{15} \approx 0.77$, suggesting that the effect of the other gases present in air is substantial, as predicted by a hard-sphere Enskog theory for multicomponent mixtures [*Kincaid et al.*, 1987].

[32] For ^{18}O of O_2, we obtain $\Omega^{18}/\Omega^{15} = 0.832 \pm 0.03$ from Siple Dome and 0.811 ± 0.03 from summer South Pole. These values may be useful in making needed corrections to records of paleoatmospheric ^{18}O of O_2 from ice cores ($\delta^{18}O_{atm}$). If the trapped gases are thermally fractionated, as during abrupt climate change, a small error results if $\delta^{15}N$ is assumed to reflect gravity alone. For example, Greenland $\delta^{15}N_{therm}$

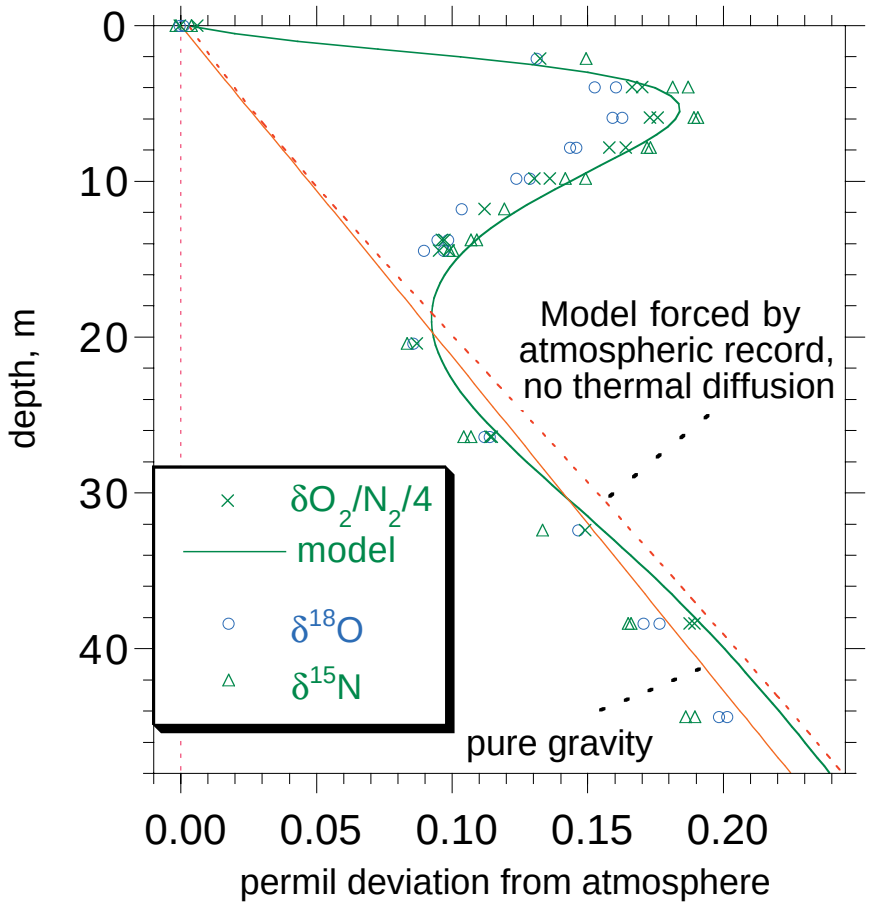

Figure 7. Observed Siple Dome $\delta O_2/N_2/4$ compared with model runs forced by atmospheric $\delta O_2/N_2/4$ as an upper boundary condition, in addition to temperature forcing. The model result is used to correct the data for atmospheric change in order to estimate the thermal diffusion sensitivity of $\delta O_2/N_2/4$ (see text).

is typically +0.15‰ after an abrupt interstadial warming event [*Severinghaus and Brook*, 1999]. The corresponding $\delta^{18}O_{therm}$ would be $0.83 \times 0.15 \times \Delta m = 0.249‰$, compared with 0.300‰ if gravity alone were acting on the gases. Existing records of $\delta^{18}O_{atm} = \delta^{18}O_{obs} - \Delta m \times \delta^{15}N_{obs}$ may therefore be biased downward by 0.05‰ at this type of event.

[33] For Kr/Ar we obtain $\Omega^{84}/\Omega^{15} = 0.333 \pm 0.03$ at Siple Dome and 0.343 ± 0.03 at South Pole in summer (0.340 ± 0.04 in winter). This observationally based value is substantially higher than the value used in the model, 0.288, which was derived from a preliminary laboratory measurement of Ω^{84}. The same laboratory experiment gave the value of Ω^{40} noted above that yields $\Omega^{40}/\Omega^{15} = 0.647$, very close to our observational value calculated here. Thus it seems unlikely that the laboratory value of Ω^{84} is badly wrong. Another possibility is that Kr behaves differently in snow than in the laboratory. More work is needed to sort out this discrepancy.

[34] For O_2/N_2 the calculation is complicated by the fact that the atmospheric value is not constant, owing mostly to marine photosynthesis

and respiration [*Keeling et al.*, 1996]. To correct for this effect, we forced the model with a 7 year record (1992–1999) of measured South Pole atmospheric O_2/N_2 (R. F. Keeling, written communication, 2001) as a top boundary condition. We assume that differences between Siple Dome and South Pole atmospheric O_2/N_2 are negligible. A constant 0.196‰ was added to the atmospheric data to bring the model curve into agreement with the observed surface value in our firn air data set (this difference reflects the different standard gases used by the Keeling and Bender laboratories, among other things). The resulting model curve (Figure 7) matches the data reasonably in the depth range 25–40 m, where thermal effects are small, giving confidence in the reconstruction. The model was then run without thermal diffusion or gravitational settling, this result (no larger than 0.011‰) was subtracted from the data to correct for atmospheric change, and the relative thermal diffusion sensitivities were calculated as for the other gases (Table 3). At Siple Dome in 1998, $\delta O_2/N_2/4$ is 90 ± 3% as sensitive to thermal diffusion as $\delta^{15}N$. This compares with a value of 85% obtained in laboratory experiments at this temperature (255 K) (Grachev and Severinghaus, manuscript in preparation, 2001). The calculation was not done for 1996 Siple Dome data because of the artifact discussed above, nor for South Pole because the experimental technique for these data was not optimized for precise O_2/N_2 measurement. However, $\delta O_2/N_2/4$ appears to have roughly the same sensitivity as $\delta^{15}N$ at South Pole (Figure 5c). We caution that the relative thermal diffusion sensitivity of these two gas pairs is highly dependent on absolute temperature, as the temperature dependences of the two Ωs have opposite signs.

6. Conclusions

[35] Air withdrawn from the snowpack (firn) at polar sites consistently shows anomalous isotope ratios in the top 5–15 m. These anomalies have the distinguishing characteristic that fractionation of different isotope pairs is not in proportion to the mass difference as it is for gravitational fractionation. Rather, fractionation tends to be proportional to the fractional mass difference $\Delta m/m$, and some differences in fractionation are not explained by mass at all. To better understand this phenomenon, we sampled air from the shallow firn at two sites, Siple Dome and South Pole, at high depth resolution. We propose that these anomalies are due to thermal diffusion, the physical process whereby a gas mixture in the presence of a temperature gradient tends to unmix, with the heavier molecules generally migrating toward colder regions. Numerical diffusion model predictions of the gas composition as a function of depth roughly agree with the observations in some instances but not in others, lending qualitative support to the hypothesis but leaving some questions unanswered. At Siple Dome in 1996, the model overpredicts the gas anomalies by ~30%. At Siple Dome in 1998, the temperature model fails to predict the measured temperature profile, suggesting a flaw in either the heat model or the temperature history used to drive the model, which was (nonideally) measured at 3 m above the snow surface. The fact that these models have no adjustable parameters makes their limited success more significant, however.

[36] A wintertime sampling confirmed the prediction that a negative isotope anomaly would appear when the near-surface temperature gradient changed sense. The strong negative anomaly (greater even than the model prediction) is firm evidence against a rectifier due to wind pumping or other seasonally varying convection. Such seasonal phenomena could create a rectifier effect by erasing the negative isotope anomaly and biasing the deep firn air and hence the ice core record of gas isotopes. Other arguments based on the match of the

deep firn gas (not shown here) to a pure diffusion model suggest that convection is negligible on longer timescales and that the seasonal thermal fractionation signals effectively cancel each other. In short, no evidence for a rectifier effect could be found.

[37] Finally, we calculate the relative thermal diffusion sensitivities from the relative amplitudes of the anomalies. Argon isotopes are fractionated 66 ± 2% and 64 ± 2% as much as nitrogen isotopes, on a per mass unit basis, at Siple Dome and South Pole, respectively. This is similar to a laboratory-derived value obtained by equilibrating air in a known temperature gradient and suggests that conditions in the firn are well approximated by laboratory studies. These estimates of relative thermal diffusion sensitivities may be helpful in calibrating the thermal diffusion paleotemperature indicator because the absolute thermal diffusion sensitivities of these gas pairs are not as well known as that of $\delta^{15}N$ and may be readily calculated from the absolute thermal diffusion sensitivity of $\delta^{15}N$. Reconstructed atmospheric histories based on firn air depth profiles should take into consideration thermal fractionation from seasonal temperature change and geothermal gradients (which exist in thinner ice sheets) as a potential source of bias.

Acknowledgments

[38] Michael Bender, Todd Sowers, Ed Brook, Richard Alley, and Ralph Keeling contributed key ideas to this work. Boaz Luz developed the $^{40}Ar/^{36}Ar$ analysis technique for air samples. We thank James Butler for inviting J.P.S. to do a wintertime sampling at the South Pole using NOAA/CMDL resources and Nathan Hill of NOAA/CMDL for taking the samples at the South Pole. Julie Palais of NSF-OPP kindly made the South Pole travel possible. We thank Michael Bender for hosting J.P.S. in his laboratory at the University of Rhode Island and supporting the Siple Dome sampling under NSF grant OPP 9117969. We thank Ken Taylor and Gregg Lamorey, Science Coordination Office, for their efforts at Siple Dome. Earl Ramsey, Jerome Brown, and Sue Root did the drilling at Siple Dome. Antarctic Support Associates staff provided sand for the backfill. Taylor Ellis of the University of Rhode Island made the Siple Dome $\delta^{15}N$ measurements, and Joe Orchardo of the University of Rhode Island provided critical technical support. Ulrike Seibt made the SIO $\delta^{18}O$ measurements. Surface temperature data are from the Automatic Weather Station Project run by Charles R. Stearns at the University of Wisconsin-Madison, which is funded by the National Science Foundation. J.P.S. was supported by a NOAA Climate and Global Change Postdoctoral Fellowship from 1995 to 1997. Further support came from NSF grant OPP 9725305 (to J.P.S.).

References

Albert, M., E. Shultz, and F. Perron, Snow and firn permeability at Siple Dome, Antarctica, *Ann. Glaciol.*, *31*, 353–356, 2000.

Alley, R. B., and B. R. Koci, Recent warming in central Greenland?, *Ann. Glaciol.*, *14*, 6–8, 1990.

Battle, M., et al., Atmospheric gas concentrations over the past century measured in air from firn at the South Pole, *Nature*, *383*, 231–235, 1996.

Bender, M. L., T. Sowers, J.-M. Barnola, and J. Chappellaz, Changes in the O_2/N_2 ratio of the atmosphere during recent decades reflected in the composition of air in the firn at Vostok Station, Antarctica, *Geophys. Res. Lett.*, *21*, 189–192, 1994a.

Bender, M. L., P. P. Tans, J. T. Ellis, J. Orchardo, and K. Habfast, A high precision isotope ratio mass spectrometry method for measuring the O_2/N_2 ratio of air, *Geochim. Cosmochim. Acta*, *58*, 4751–4758, 1994b.

Butler, J. H., M. Battle, M. L. Bender, S. A. Montzka, A. D. Clarke, E. S. Saltzman, C. M. Sucher, J. P. Severinghaus, and J. W. Elkins, A record of atmospheric halocarbons during the twentieth century from polar firn air, *Nature*, *399*, 749–755, 1999.

Chapman, S., and F. W. Dootson, A note on thermal diffusion, *Philos. Mag.*, *33*, 248–253, 1917.

Colbeck, S. C., Air movement in snow due to windpumping, *J. Glaciol.*, *35*, 209–213, 1989.

Connolley, W. M., The Antarctic temperature inversion, *Int. J. Climatol.*, *16*, 1333–1342, 1996.

Craig, H., Y. Horibe, and T. Sowers, Gravitational separation of gases and isotopes in polar ice caps, *Science*, *242*, 1675–1678, 1988.

Fabre, A., J.-M. Barnola, L. Arnaud, and J. Chappellaz, Determination of gas diffusivity in polar firn: Comparison between experimental measurements and inverse modeling, *Geophys. Res. Lett.*, *27*, 557–560, 2000.

Francey, R. J., M. R. Manning, C. E. Allison, S. A. Coram, D. M. Etheridge, R. L. Langenfelds, D. C. Lowe,

and L. P. Steele, A history of delta C-13 in atmospheric CH_4 from the Cape Grim air archive and Antarctic firn air, *J. Geophys. Res.*, *104*, 23,631–23,643, 1999.

Gibbs, J. W., On the equilibrium of heterogeneous substances, in *The Collected Works of J. Willard Gibbs*, vol. I, *Thermodynamics*, pp. 158–159, Copp, Clark, Mississauga, Ont., Canada, 1928.

Grew, K. E., and T. L. Ibbs, *Thermal Diffusion in Gases*, Cambridge Univ. Press, New York, 1952.

Herron, M. M., and C. C. Langway, Firn densification: An empirical model, *J. Glaciol.*, *25*, 373–385, 1980.

Keeling, R. F., S. C. Piper, and M. Heimann, Global and hemispheric CO_2 sinks deduced from changes in atmospheric O_2 concentration, *Nature*, *381*, 218–221, 1996.

Kincaid, J. M., E. G. D. Cohen, and M. Lopez de Haro, The Enskog theory for multicomponent mixtures, IV, Thermal diffusion, *J. Chem. Phys.*, *86*, 963–975, 1987.

Lang, C., M. Leuenberger, J. Schwander, and S. Johnsen, 16°C rapid temperature variation in central Greenland 70,000 years ago, *Science*, *286*, 934–937, 1999.

Leuenberger, M., J. Schwander, and C. Lang, Delta 15 N measurements as a calibration tool for the paleothermometer and gas-ice age differences: A case study for the 8200 B.P. event on GRIP ice, *J. Geophys. Res.*, *104*, 22,163–22,170, 1999.

Leuenberger, M., J. Schwander, R. Mulvaney, and P. Nyfeler, Experimental and theoretical calculation of thermal diffusion factors, Newsletter, European Geophysical Society Scientific Programme, No. 74, p. 207, March 2000.

Lindemann, F. A., and F. W. Aston, The possibility of separating isotopes, *Philos. Mag. Ser. 6*, *37*, 523–534, 1919.

Paterson, W. S. B., *The Physics of Glaciers*, Pergamon, New York, 1969.

Powers, D., K. O'Neill, and S. C. Colbeck, Theory of natural convection in snow, *J. Geophys. Res.*, *90*, 10,641–10,649, 1985.

Reid, R. C., J. M. Prausnitz, and T. K. Sherwood, *The Properties of Gases and Liquids*, 3rd ed., McGraw-Hill, New York, 1977.

Schwander, J., The transformation of snow to ice and the occlusion of gases, in *The Environmental Record in Glaciers and Ice Sheets*, edited by H. Oeschger and C. C. Langway Jr., pp. 53–67, John Wiley, New York, 1989.

Schwander, J., B. Stauffer, and A. Sigg, Air mixing in firn and the age of the air at pore close-off, *Ann. Glaciol.*, *10*, 141–145, 1988.

Schwander, J., J.-M. Barnola, C. Andrie, M. Leuenberger, A. Ludin, D. Raynaud, and B. Stauffer, The age of the air in the firn and the ice at Summit, Greenland, *J. Geophys. Res.*, *98*, 2831–2838, 1993.

Severinghaus, J. P., and E. J. Brook, Abrupt climate change at the end of the last glacial period inferred from trapped air in polar ice, *Science*, *286*, 930–934, 1999.

Severinghaus, J. P., and E. J. Brook, Do atmospheric gases fractionate during air bubble closure in polar firn and ice? (abstract), *Eos Trans. AGU*, *81*(19), Spring Meet. Suppl., S20, 2000.

Severinghaus, J. P., M. L. Bender, R. F. Keeling, and W. S. Broecker, Fractionation of soil gases by diffusion of water vapor, gravitational settling, and thermal diffusion, *Geochim. Cosmochim. Acta*, *60*, 1005–1018, 1996.

Severinghaus, J. P., R. F. Keeling, B. R. Miller, R. F. Weiss, B. Deck, and W. S. Broecker, Feasibility of using sand dunes as archives of old air, *J. Geophys. Res.*, *102*, 16,783–16,792, 1997.

Severinghaus, J. P., T. Sowers, E. J. Brook, R. B. Alley, and M. L. Bender, Timing of abrupt climate change at the end of the Younger Dryas period from thermally fractionated gases in polar ice, *Nature*, *391*, 141–146, 1998.

Sowers, T., M. L. Bender, and D. Raynaud, Elemental and isotopic composition of occluded O_2 and N_2 in polar ice, *J. Geophys. Res.*, *94*, 5137–5150, 1989.

Sowers, T., M. L. Bender, D. Raynaud, and Y. S. Korotkevich, $\delta^{15}N$ of N_2 in air trapped in polar ice: A tracer of gas transport in the firn and a possible constraint on ice age-gas age differences, *J. Geophys. Res.*, *97*, 15,683–15,697, 1992.

Trudinger, C. M., I. G. Enting, D. M. Etheridge, R. J. Francey, V. A. Levchenko, L. P. Steele, D. Raynaud, and L. Arnaud, Modeling air movement and bubble trapping in firn, *J. Geophys. Res.*, *102*, 6747–6763, 1997.